

# Theory of Telecommunications Networks

Anton Čižmár  
Ján Papaj



# CONTENTS

|   |           |
|---|-----------|
| <b>Preface</b> .....  | <b>5</b>  |
| <b>1 Introduction</b> .....   | <b>6</b>  |
| 1.1 <i>Mathematical models for communication channels</i> .....                         | 8         |
| 1.2 <i>Channel capacity for digital communication</i> .....                             | 10        |
| 1.2.1 <i>Shannon Capacity and Interpretation</i> .....                                  | 10        |
| 1.2.2 <i>Hartley Channel Capacity</i> .....   | 12        |
| 1.2.3 <i>Solved Problems</i> .....  | 13        |
| 1.3 <i>Noise in digital communication system</i> .....                                  | 15        |
| 1.3.1 <i>White Noise</i> .....  | 17        |
| 1.3.2 <i>Thermal Noise</i> .....  | 18        |
| 1.3.3 <i>Solved Problems</i> .....  | 19        |
| 1.4 <i>Summary</i> .....  | 20        |
| 1.5 <i>Exercises</i> .....  | 21        |
| <b>2 Signal and Spectra</b> .....   | <b>23</b> |
| 2.1 <i>Deterministic and random signals</i> .....                                       | 23        |
| 2.2 <i>Periodic and nonperiodic signals</i> .....                                       | 23        |
| 2.3 <i>Analog and discrete Signals</i> .....  | 23        |
| 2.4 <i>Energy and power Signals</i> .....   | 23        |
| 2.5 <i>Spectral Density</i> .....   | 25        |
| 2.5.1 <i>Energy Spectral Density</i> .....  | 25        |
| 2.5.2 <i>Power Spectral Density</i> .....   | 25        |
| 2.5.3 <i>Solved Problems</i> .....  | 26        |
| 2.6 <i>Autocorrelation</i> .....  | 27        |
| 2.6.1 <i>Autocorrelation of an Energy Signal</i> .....                                  | 27        |
| 2.6.2 <i>Autocorrelation of a Periodic Signal</i> .....                                 | 27        |
| 2.7 <i>Baseband versus Bandpass</i> .....   | 28        |
| 2.8 <i>Summary</i> .....  | 29        |
| 2.9 <i>Exercises</i> .....  | 30        |
| <b>3 Probability and stochastic processes</b> .....                                     | <b>31</b> |
| 3.1 <i>Probability</i> .....  | 31        |
| 3.1.1 <i>Joint Events and Joint Probabilities</i> .....                                 | 31        |
| 3.1.2 <i>Conditional Probabilities</i> .....  | 32        |
| 3.1.3 <i>Statistical Independence</i> .....   | 33        |
| 3.1.4 <i>Solved Problems</i> .....  | 33        |
| 3.2 <i>Random Variables, Probability Distributions, and probability Densities</i> ..... | 36        |
| 3.2.1 <i>Statistically Independent Random Variables</i> .....                           | 37        |

|          |  |           |
|----------|--|-----------|
| 3.2.2    | <i>Statistical Averages of Random Variables</i> .....                                      | 37        |
| 3.2.3    | <i>Some Useful Probability Distributions</i> .....   | 38        |
| 3.3      | <i>Stochastic processes</i> .....  | 41        |
| 3.3.1    | <i>Stationary Stochastic Processes</i> .....   | 41        |
| 3.3.2    | <i>Statistical Averages</i> .....  | 41        |
| 3.3.3    | <i>Power Density Spectrum</i> .....  | 43        |
| 3.3.4    | <i>Response of a Linear Time-Invariant System (channel) to a Random Input Signal</i> ..... | 43        |
| 3.3.5    | <i>Sampling Theorem for Band-Limited Stochastic Processes</i> .....                        | 44        |
| 3.3.6    | <i>Discrete-Time Stochastic Signals and Systems</i> .....                                  | 45        |
| 3.3.7    | <i>Cyclostationary Processes</i> .....   | 46        |
| 3.3.8    | <i>Solved Problems</i> .....   | 47        |
| 3.4      | <i>Summary</i> .....   | 50        |
| 3.5      | <i>Exercises</i> .....   | 52        |
| <b>4</b> | <b>Signal space concept</b> .....  | <b>55</b> |
| 4.1      | <i>Representation Of Band-Pass Signals And Systems</i> .....                               | 55        |
| 4.1.1    | <i>Representation of Band-Pass Signals</i> .....   | 55        |
| 4.1.2    | <i>Representation of Band-Pass Stationary Stochastic Processes</i> .....                   | 58        |
| 4.2      | <i>Introduction of the Hilbert transform</i> .....   | 59        |
| 4.3      | <i>Different look at the Hilbert transform</i> .....                                       | 59        |
| 4.3.1    | <i>Hilbert Transform, Analytic Signal and the Complex Envelope</i> .....                   | 59        |
| 4.3.2    | <i>Hilbert Transform in Frequency Domain</i> .....   | 61        |
| 4.3.3    | <i>Hilbert Transform in Time Domain</i> .....  | 62        |
| 4.3.4    | <i>Analytic Signal</i> .....   | 64        |
| 4.3.5    | <i>Solved Problems</i> .....   | 66        |
| 4.4      | <i>Signal Space Representation</i> .....   | 69        |
| 4.4.1    | <i>Vector Space Concepts</i> .....   | 69        |
| 4.4.2    | <i>Signal Space Concepts</i> .....   | 70        |
| 4.4.3    | <i>Orthogonal Expansions of Signals</i> .....  | 70        |
| 4.4.4    | <i>Gram-Schmidt procedure</i> .....  | 71        |
| 4.4.5    | <i>Solved Problems</i> .....   | 74        |
| 4.4.6    | <i>Summary</i> .....   | 78        |
| 4.5      | <i>Exercises</i> .....   | 79        |
| <b>5</b> | <b>Digital modulation schemes</b> .....  | <b>82</b> |
| 5.1      | <i>Signal Space Representation</i> .....   | 82        |
| 5.2      | <i>Memoryless Modulation Methods</i> .....   | 82        |
| 5.2.1    | <i>Pulse-amplitude-modulated (PAM) signals (ASK)</i> .....                                 | 83        |

|          |  |            |
|----------|--|------------|
| 5.2.2    | <i>Phase-modulated signal (PSK)</i> .....                                  | 85         |
| 5.2.3    | <i>Quadrature Amplitude Modulation (QAM)</i> .....                         | 86         |
| 5.3      | <i>Multidimensional Signals</i> .....                                      | 88         |
| 5.3.1    | <i>Orthogonal multidimensional signals</i> .....                           | 88         |
| 5.3.2    | <i>Linear Modulation with Memory</i> .....                                 | 92         |
| 5.3.3    | <i>Non-Linear Modulation Methods with Memory</i> .....                     | 95         |
| 5.4      | <i>Spectral Characteristic Of Digitally Modulated Signals</i> .....        | 101        |
| 5.4.1    | <i>Power Spectra of Linearly Modulated Signals</i> .....                   | 101        |
| 5.4.2    | <i>Power Spectra of CPFSK and CPM Signals</i> .....                        | 102        |
| 5.4.3    | <i>Solved Problems</i> .....   | 106        |
| 5.5      | <i>Summary</i> .....   | 110        |
| 5.6      | <i>Exercises</i> .....   | 110        |
| <b>6</b> | <b>Optimum Receivers for the AWGN Channel</b> .....                        | <b>113</b> |
| 6.1      | <i>Optimum Receivers For Signals Corrupted By Awgn</i> .....               | 113        |
| 6.1.1    | <i>Correlation demodulator</i> .....                                       | 114        |
| 6.1.2    | <i>Matched-Filter demodulator</i> .....                                    | 116        |
| 6.1.3    | <i>The Optimum detector</i> .....  | 118        |
| 6.1.4    | <i>The Maximum-Likelihood Sequence Detector</i> .....                      | 120        |
| 6.2      | <i>Performance Of The Optimum Receiver For Memoryless Modulation</i> ..... | 123        |
| 6.2.1    | <i>Probability of Error for Binary Modulation</i> .....                    | 123        |
| 6.2.2    | <i>Probability of Error for M-ary Orthogonal Signals</i> .....             | 126        |
| 6.2.3    | <i>Probability of Error for M-ary Biorthogonal Signals</i> .....           | 127        |
| 6.2.4    | <i>Probability of Error for Simplex Signals</i> .....                      | 129        |
| 6.2.5    | <i>Probability of Error for M-ary Binary-Coded Signals</i> .....           | 129        |
| 6.2.6    | <i>Probability of Error for M-ary PAM</i> .....                            | 130        |
| 6.2.7    | <i>Probability of Error for M-ary PSK</i> .....                            | 130        |
| 6.2.8    | <i>Probability of Error for QAM</i> .....                                  | 132        |
| 6.3      | <i>Solved Problems</i> .....   | 134        |
| 6.4      | <i>Summary</i> .....   | 141        |
| 6.5      | <i>Exercises</i> .....   | 142        |
| <b>7</b> | <b>Performance analysis of digital modulations</b> .....                   | <b>144</b> |
| 7.1      | <i>Goals Of The Communications System Designer</i> .....                   | 144        |
| 7.2      | <i>Error Probability Plane</i> .....                                       | 144        |
| 7.3      | <i>Nyquist Minimum Bandwidth</i> .....                                     | 146        |
| 7.4      | <i>Shannon-Hartley Capacity Theorem</i> .....                              | 146        |
| 7.4.1    | <i>Shannon Limit</i> .....   | 148        |
| 7.5      | <i>Bandwidth-Efficiency Plane</i> .....                                    | 150        |

|                         |  |            |
|-------------------------|--|------------|
| 7.5.1                   | <i>Bandwidth Efficiency of MPSK and MFSK Modulation</i> .....                    | 151        |
| 7.5.2                   | <i>Analogies Between Bandwidth-Efficiency and Error-Probability Planes</i> ..... | 152        |
| 7.6                     | <i>Modulation And Coding Trade-Offs</i> .....                                    | 153        |
| 7.7                     | <i>Defining, Designing, And Evaluating Digital Communication Systems</i> .....   | 154        |
| 7.7.1                   | <i>M-ary Signaling</i> .....   | 154        |
| 7.7.2                   | <i>Bandwidth-Limited Systems</i> .....   | 155        |
| 7.7.3                   | <i>Power-Limited Systems</i> .....   | 156        |
| 7.7.4                   | <i>Requirements for MPSK and MFSK Signaling</i> .....                            | 157        |
| 7.7.5                   | <i>Bandwidth-Limited Uncoded System Example</i> .....                            | 158        |
| 7.7.6                   | <i>Power-Limited Uncoded System Example</i> .....                                | 160        |
| 7.8                     | <i>Solved Problems</i> .....   | 162        |
| 7.9                     | <i>Summary</i> .....   | 165        |
| 7.10                    | <i>Exercise</i> .....  | 166        |
| <b>8</b>                | <b>Why use error-correction coding</b> .....                                     | <b>167</b> |
| 8.1                     | <i>Trade-Off 1: Error Performance versus Bandwidth</i> .....                     | 167        |
| 8.2                     | <i>Trade-Off 2: Power versus Bandwidth</i> .....                                 | 168        |
| 8.3                     | <i>Coding Gain</i> .....   | 168        |
| 8.4                     | <i>Trade-Off 3: Data Rate versus Bandwidth</i> .....                             | 168        |
| 8.5                     | <i>Trade-Off 4: Capacity versus Bandwidth</i> .....                              | 169        |
| 8.6                     | <i>Code Performance at Low Values of <math>E_b/N_0</math></i> .....              | 169        |
| 8.7                     | <i>Solved problem</i> .....  | 170        |
| 8.8                     | <i>Exercise</i> .....  | 171        |
| <b>Appendix A</b>       | .....  | <b>173</b> |
|                         | <i>The Q-function</i> .....  | 173        |
|                         | <i>The Error Function</i> .....  | 174        |
| <b>Appendix B</b> ..... |  | <b>175</b> |
|                         | <i>Comparison of M-ary signaling techniques</i> .....                            | 175        |
|                         | <i>Error performance of M-ary signaling techniques</i> .....                     | 175        |
| <b>References</b> ..... |  | <b>176</b> |

## **PREFACE**

Providing the theory of digital communication systems, this textbook prepares senior undergraduate and graduate students for the engineering practices required in the real world.

With this textbook, students can understand how digital communication systems operate in practice, learn how to design subsystems, and evaluate end-to-end performance.

The book contains many examples to help students achieve an understanding of the subject. The problems at the end of each chapter follow closely the order of the sections.

The entire book is suitable for one semester course in digital communication.

All materials for teaching texts were drawn from sources listed in References.

## 5 DIGITAL MODULATION SCHEMES

The digital data are usually in the form of a stream of binary data, i.e., a sequence of 0s and 1s. Regardless of whether these data are inherently digital (for instance, the output of a computer terminal generating ASCII code) or the result of analog-to-digital conversion of an analog source (for instance, digital audio and video), the goal is to reliably transmit these data to the destination by using the given communication channel.

Depending on the nature of the communication channel, data can suffer from one or more of certain channel impairments including noise, attenuation, distortion, fading, and interference. To transmit the binary stream over the communication channel, we need to generate a signal that represents the binary data stream and matches the characteristics of the channel. This signal should represent the binary data, meaning that we should be able to retrieve the binary stream from the signal; and it should match the characteristics of the channel, meaning that its bandwidth should match the bandwidth of the channel, and it should be able to resist the impairments caused by the channel. Since different channels cause different types of impairments, signals designed for these channels can be drastically different. The process of mapping a digital sequence to signals for transmission over a communication channel is called digital modulation or digital signaling.

In the process of modulation, usually the transmitted signals are bandpass signals suitable for transmission in the bandwidth provided by the communication channel. In this chapter we study the most commonly used modulation schemes and their properties.

### 5.1 SIGNAL SPACE REPRESENTATION

In the transmission of digital information over a communication channel, the modulator is the interface device that maps the digital information into analog waveforms that match the characteristics of the channel. The mapping is generally performed by taking blocks of  $b = \log_2 M$  binary digits at a time from the information sequence  $\{a_n\}$  and selecting one of  $M = 2^b$  deterministic, finite energy waveforms  $\{s_m(t), m = 1, 2, \dots, M\}$  for transmission over the channel.

- *Modulator with memory* – when the mapping from the digital sequence  $\{a_n\}$  to waveforms is performed under constraint that a waveform transmitted in any time interval depends on one or more previously transmitted waveforms.
- *Memoryless modulator* – when the mapping from the sequence  $\{a_n\}$  to the waveforms  $\{s_m(t)\}$  is performed without any constraints on previously transmitted waveforms.
- *Linear modulator* – principle of superposition
- *Non-linear modulator* - principle of superposition does not exist

### 5.2 MEMORYLESS MODULATION METHODS

The waveforms  $s_m(t)$  used to transmit information over the communication channel can be, in general, of any form. However, usually these waveforms are bandpass signals which may differ in amplitude or phase or frequency, or some combination of two or more signal parameters. We consider following signals:

- *Digital Pulse Amplitude Modulated (PAM) signals (ASK)*
- *Phase-modulated signal (PSK)*
- *Quadrature Amplitude Modulation (QAM)*



### 5.2.1 Pulse-amplitude-modulated (PAM) signals (ASK)

In digital PAM, the signal waveforms may be represented as

$$s_m(t) = \text{Re}[A_m g(t) e^{j2\pi f_c t}] = A_m g(t) \cos 2\pi f_c t; \quad m = 1, 2, \dots, M \quad (5.1)$$

where  $\{A_m, 1 \leq m \leq M\}$  denote the set of  $M$  possible amplitudes corresponding to  $M = 2^k$  possible  $k$ -bit block of symbols.

The signal amplitudes take the discrete values (levels)

$$A_m = (2m - 1 - M)d, \quad m = 1, 2, \dots, M \quad (5.2)$$

where  $2d$  is the distance between adjacent signal amplitudes. The waveform  $g(t)$  is a real-valued signal pulse whose shape influences the spectrum of the transmitted signal. The symbol rate for the PAM is  $R/k$ . This is the rate at which changes occur in the amplitude of the carrier to reflect the transmission of new information. The time interval  $T_b = 1/R$  is called the bit interval and the time interval  $T = k/R$  is called the symbol interval.

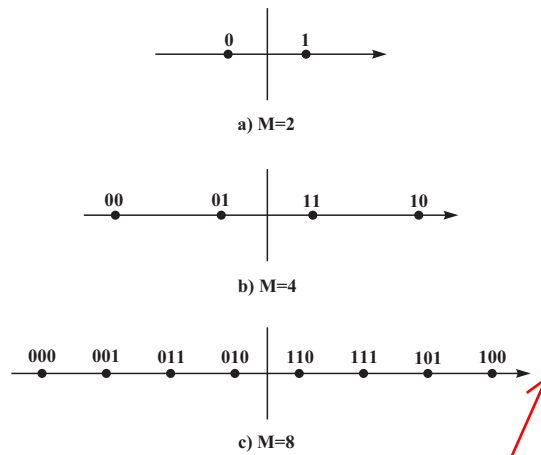


Figure 5.1 Signal space diagram for digital PAM signals

The  $M$  PAM signals have energies

$$E_m = \int_0^T s_m^2(t) dt = \frac{1}{2} A_m^2 \int_0^T g^2(t) dt = \frac{1}{2} A_m^2 E_g \quad (5.3)$$

where  $E_g$  denotes the energy in the pulse  $g(t)$ .

These signals are one-dimensional ( $N=1$ ) and are represented by the general form

$$s_m(t) = s_m f(t) \quad (5.4)$$

where  $f(t)$  is defined as the unit-energy signal waveform given as

$$f(t) = \sqrt{\frac{2}{E_g}} g(t) \cos 2\pi f_c t \quad (5.5)$$

And



$$s_m = A_m \sqrt{\frac{1}{2} E_g}; m = 1, 2, \dots, M \quad (5.6)$$

The corresponding signal space diagram for  $M=2$ ,  $M=4$ , and  $M=8$  are shown in Figure 5.1. Digital PAM is also called *amplitude-shift keying (ASK)*. Gray encoding mapping of the bits.

Euclidean distance between any pair of signal points is

$$d_{mn}^{(e)} = \sqrt{(s_m - s_n)^2} = \sqrt{\frac{1}{2} E_g} |A_m - A_n| = d \sqrt{2 E_g} |m - n| \quad (5.7)$$

and the *minimum Euclidean distance* is

$$d_{min}^{(e)} = d \sqrt{2 E_g} \quad (5.8)$$

The carrier-modulated PAM signal represented by Equation 5.1 is a double-sideband (DSB) signal and requires twice the channel bandwidth of the equivalent low-pass signal for transmission.

The digital PAM signal is also appropriate for transmission over a channel that does not require carrier modulation. In this case the signal is called *baseband signal* represented as

$$s_m(t) = A_m g(t); m = 1, 2, \dots, M \quad (5.9)$$

If  $M=2$  than such signals are called *antipodal signal* with property

$$s_1(t) = -s_2(t) \quad (5.10)$$

And crosscorrelation coefficient of -1.

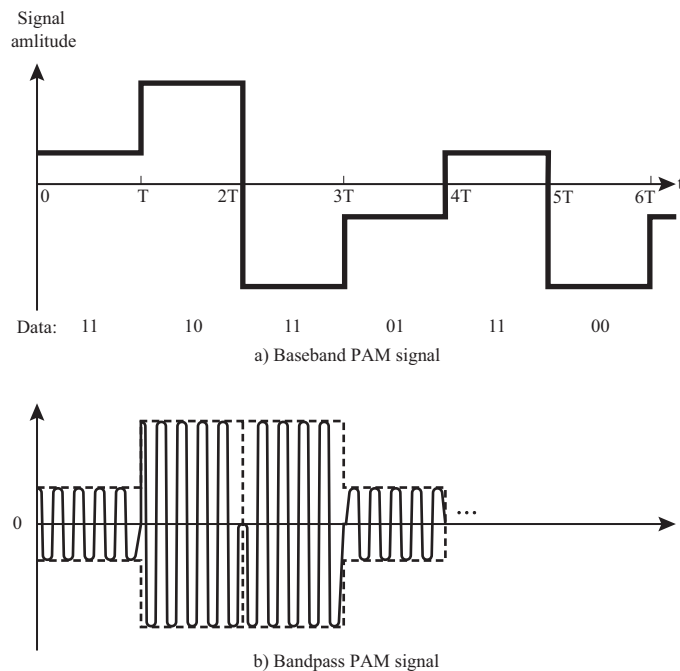


Figure 5.2 Baseband and band-pass PAM signals

### 5.2.2 Phase-modulated signal (PSK)

In digital phase modulation, the M signal waveforms are represented as

$$\begin{aligned}
 s_m(t) &= \text{Re} \left[ g(t) e^{j2\pi \frac{(m-1)}{M}} e^{j2\pi f_c t} \right] \\
 &= g(t) \cos \left[ 2\pi f_c t + \frac{2\pi}{M} (m-1) \right] \\
 &= g(t) \cos \frac{2\pi}{M} (m-1) \cos 2\pi f_c t - g(t) \sin \frac{2\pi}{M} (m-1) \sin 2\pi f_c t, \quad m = 1, 2, \dots, M \quad (5.11)
 \end{aligned}$$

where  $g(t)$  is the signal pulse shape and  $\Theta_m = \frac{2\pi(m-1)}{M}$ ,  $m = 1, 2, \dots, M$  are the M possible phases of the carrier.

These signal waveforms have equal energy

$$E = \int_0^T s_m^2(t) dt = \frac{1}{2} \int_0^T g^2(t) dt = \frac{1}{2} E_g \quad (5.12)$$

Furthermore, the signal waveforms may be represented as linear combination of two orthonormal signal waveforms  $f_1(t)$  and  $f_2(t)$

$$s_m(t) = s_{m1} f_1(t) + s_{m2} f_2(t) \quad (5.13)$$

where

$$f_1(t) = \sqrt{\frac{2}{E_g}} g(t) \cos 2\pi f_c t \quad (5.14)$$

$$f_2(t) = -\sqrt{\frac{2}{E_g}} g(t) \sin 2\pi f_c t \quad (5.15)$$

and the two-dimensional vectors  $s_m = [s_{m1} s_{m2}]$  are given by

$$s_m = \left[ \sqrt{\frac{E_g}{2}} \cos 2\pi \frac{(m-1)}{M}; \sqrt{\frac{E_g}{2}} \sin 2\pi \frac{(m-1)}{M} \right] \quad (5.16)$$

If M=2

$$s_1 = \left[ \sqrt{\frac{E_g}{2}}; 0 \right]$$

$$s_2 = \left[ -\sqrt{\frac{E_g}{2}}; 0 \right]$$

Signal space diagrams for M=2, 4, 8 are shown in Figure 5.3. We note that M=2 corresponds to one-dimensional signals, which are identical to binary PAM signals.

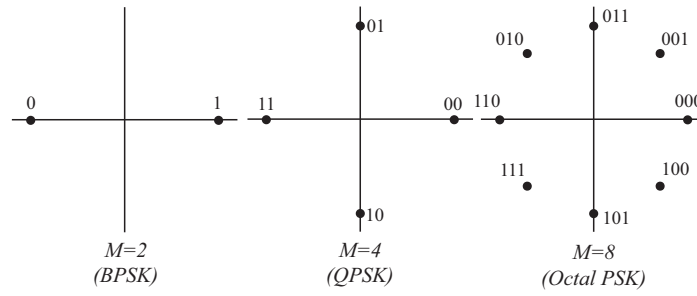


Figure 5.3 Signal space diagram for PSK signals

The Euclidean distance (ED) between any pair of signal points

$$d_{mn}^{(e)} = \|s_m - s_n\| = \{E_g [1 - \cos \frac{2\pi}{M}(m - n)]\}^{\frac{1}{2}} \quad (5.17)$$

The minimum ED corresponds to the case in which  $|m - n| = 1$ , i.e., adjacent signal phases. In this case,

$$d_{mn}^{(e)} = \sqrt{E_g (1 - \cos \frac{2\pi}{M})} \quad (5.18)$$

A variant of 4-phase PSK (QPSK), called  $\frac{\pi}{4}$ -QPSK is obtained by introducing an additional  $\frac{\pi}{4}$  phase shift in the carrier phase in each symbol interval. This phase shift facilitates symbol synchronization.

### 5.2.3 Quadrature Amplitude Modulation (QAM)

The bandwidth efficiency of PAM/SSB can also be obtained by simultaneously impressing two separate  $k$ -bit symbols from the information sequence  $\{a_n\}$  on two quadrature carriers  $\cos$  and  $\sin$ . The resulting modulation technique is called QAM, and the corresponding signal waveforms is expressed as

$$\begin{aligned} s_m(t) &= \text{Re}[(A_{mc} + jA_{ms})g(t)e^{j2\pi f_c t}] \\ &= A_{mc}g(t) \cos 2\pi f_c t - A_{ms}g(t) \sin 2\pi f_c t, \quad m = 1, 2, \dots, M \end{aligned} \quad (5.19)$$

where  $A_{mc}$  and  $A_{ms}$  are the information-bearing signal amplitudes of the quadrature carriers and  $g(t)$  is the signal pulse.

Alternatively, the QAM signal waveforms may be expressed as

$$\begin{aligned} s_m(t) &= \text{Re}[V_m e^{j\Theta_m} g(t) e^{j2\pi f_c t}] \\ &= V_m g(t) \cos(2\pi f_c t + \Theta) \end{aligned} \quad (5.20)$$

Where  $V_m = \sqrt{A_{mc}^2 + A_{ms}^2}$  and  $\Theta_m = \tan^{-1}(A_{ms}/A_{mc})$ .

QAM signal waveforms may be viewed as combined amplitude and phase modulation.

As in the case of PSK signals, the QAM signal waveforms may be represented as a linear combination of two orthonormal signal waveforms

$$s_m(t) = s_{m1}f_1(t) + s_{m2}f_2(t) \quad (5.21)$$

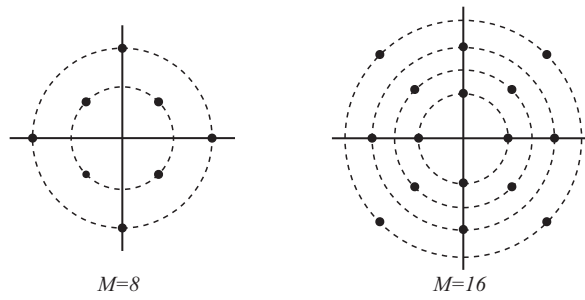


Figure 5.4 Examples of combined PAM-PSK signal space diagrams

where

$$f_1(t) = \sqrt{\frac{2}{E_g}} g(t) \cos 2\pi f_c t \quad (5.22)$$

$$f_2(t) = -\sqrt{\frac{2}{E_g}} g(t) \sin 2\pi f_c t \quad (5.23)$$

and

$$s_m = [s_{m1} s_{m2}] = \left[ A_{mc} \sqrt{\frac{E_g}{2}}; A_{ms} \sqrt{\frac{E_g}{2}} \right] \quad (5.24)$$

Euclidean distance between any pair of signal points is

$$d_{mn}^{(e)} = \|s_m - s_n\| = \sqrt{\frac{1}{2} E_g [(A_{mc} - A_{nc})^2 + (A_{ms} - A_{ns})^2]} \quad (5.25)$$

In the special case where the signal amplitudes take the set of discrete values  $\{(2m - 1 - M)d, m = 1, 2, \dots, M\}$ , the signal diagram is rectangular, as shown in Figure 5.5. In this case, the ED between adjacent points, i.e, the minimum distance is

$$d_{mn}^{(e)} = d\sqrt{2E_g} \quad (5.26)$$

which is the same result as for PAM.

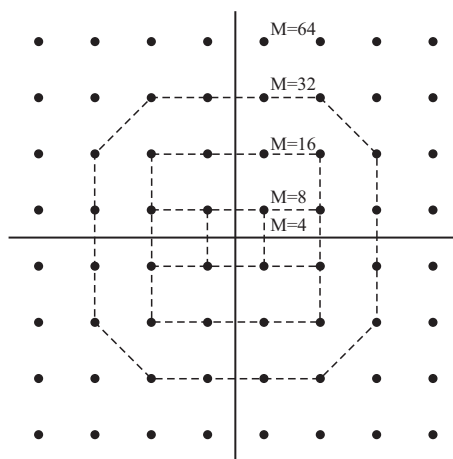


Figure 5.5 Several signal space diagram for rectangular QAM

### 5.3 MULTIDIMENSIONAL SIGNALS

It is apparent from the discussion above that the digital modulation of the carrier amplitude and phase allows us to construct signal waveforms that correspond to two-dimensional vectors and signal space diagrams. If we wish to construct signal waveforms corresponding to higher-dimensional vectors, we may use either the time domain or the frequency domain or both in order to increase the number of dimensions.

Suppose we have  $N$ -dimensional signal vectors. For any  $N$ , we may subdivide a time interval of length  $T_1 = NT$  into  $N$  subintervals of length  $T = \frac{T_1}{N}$ . In each subinterval of length  $T$ , we may use binary PAM (a one-dimensional signal) to transmit an element of the  $N$ -dimensional signal vector. Thus, the  $N$  time slots are used to transmit the  $N$ -dimensional signal vector. If  $N$  is even, a time slot of length  $T$  may be used to simultaneously transmit two components of the  $N$ -dimensional vector by modulating the amplitude of quadrature carriers independently by the corresponding components. In this manner, the  $N$ -dimensional signal vector is transmitted in  $(\frac{1}{2})NT$  seconds ( $\frac{1}{2} - N$  time slots).

Alternatively, a frequency band of width  $N\Delta f$  may be subdivided into  $N$  frequency slots each of width  $\Delta f$ . An  $N$ -dimensional signal vector can be transmitted over the channel by simultaneously modulating the amplitude of  $N$  carriers, one in each of the  $N$  frequency slots. Care must be taken to provide sufficient frequency separation  $\Delta f$  between successive carriers so that there is no cross-talk interference among signals on the  $N$  carriers. If quadrature carriers are used in each frequency slot, the  $N$ -dimensional vector (even  $N$ ) may be transmitted in  $(\frac{1}{2})N$  frequency slots, thus reducing the channel bandwidth utilization by a factor of 2.

More generally, we may use both the time and frequency domains jointly to transmit an  $N$ -dimensional signal vector. For example, Figure 5.6 illustrates a subdivision of the time and frequency axes into 12 slots. Thus, an  $N=12$  – dimensional signal vector may be transmitted by PAM or an  $N=24$  – dimensional signal vector may be transmitted by use of two quadrature carriers (QAM) in each slot.

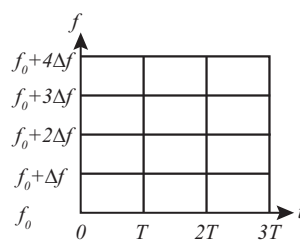


Figure 5.6 Subdivision of time and frequency axes into distinct slots

#### 5.3.1 Orthogonal multidimensional signals

##### Frequency-shift keying (FSK)

As a special case of the construction of multidimensional signals, let us consider the construction of  $M$  equal-energy orthogonal signal waveforms that differ in frequency and are represented as

$$s_m(t) = \text{Re}[s_{lm}(t)e^{j2\pi f_c t}]$$

$$= \sqrt{\frac{2E}{T}} \cos[2\pi f_c t + 2\pi m \Delta f t] \quad (5.27)$$

Where the equivalent low-pass signal waveforms are defined as

$$s_{lm}(t) = \sqrt{\frac{2E}{T}} e^{j2\pi m \Delta f t} \quad (5.28)$$

This type of frequency modulation is called **frequency-shift keying (FSK)**.

These waveforms are characterized as having equal energy and cross-correlation coefficients

$$\rho_{km} = \frac{2E/T}{2E} \int_0^T e^{j2\pi(m-k)\Delta f t} dt = \frac{\sin \pi T(m-k)\Delta f}{\pi T(m-k)\Delta f} e^{j\pi T(m-k)\Delta f} \quad (5.29)$$

The real part of  $\rho_{km}$  is

$$\begin{aligned} \rho_r &\equiv \text{Re}(\rho_{km}) = \frac{\sin[\pi T(m-k)\Delta f]}{\pi T(m-k)\Delta f} \cos[\pi T(m-k)\Delta f] \\ &= \frac{\sin[2\pi T(m-k)\Delta f]}{2\pi T(m-k)\Delta f} \end{aligned} \quad (5.30)$$

First, we observe that  $\text{Re}(\rho_{km}) = 0$  when  $\Delta f = \frac{1}{2T}$  and  $k \neq m$ . Since  $|m - k| = 1$  corresponds to adjacent frequency slots,  $\Delta f = \frac{1}{2T}$  represents the minimum frequency separation between adjacent signals for orthogonality of the M signals.

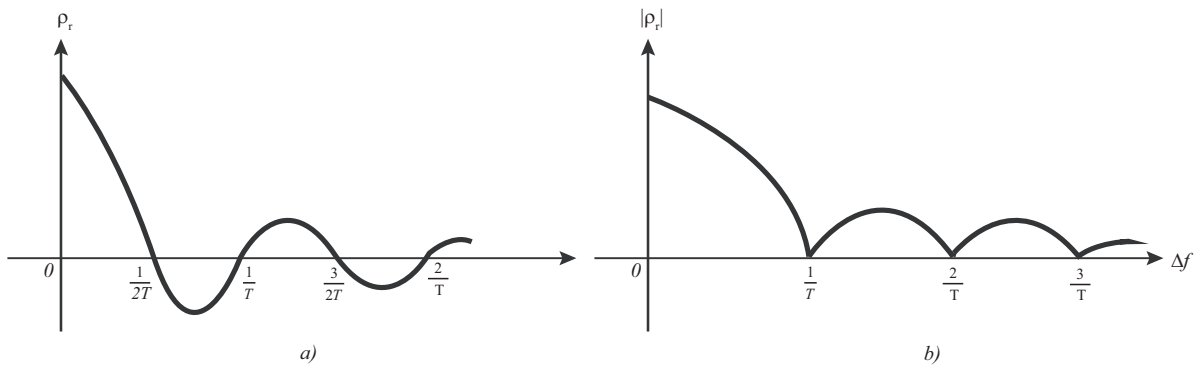


Figure 5.7 Cross-correlation coefficient as a function of frequency separation for FSK signals

Note that  $|\rho_{km}| = 0$  for multiples of  $1/T$  whereas  $\text{Re}(\rho_{km}) = 0$  for multiples of  $\frac{1}{2T}$ .

For the case in which  $\Delta f = \frac{1}{2T}$ , the M FSK signals are equivalent to the N-dimensional vectors

$$s_1 = [\sqrt{E} \ 0 \ 0 \ 0 \ \dots \ 0]$$

$$s_2 = [0 \ \sqrt{E} \ 0 \ 0 \ \dots \ 0]$$

$$s_3 = [0 \ 0 \ 0 \ \sqrt{E} \ \dots \ 0]$$

⋮

$$s_N = [0 \ 0 \ 0 \ 0 \dots \sqrt{E}] \tag{5.31}$$

where  $N = M$ . The distance between pairs of signals is

$$d_{km}^{(e)} = \sqrt{2E}, \text{ for all } m, k \tag{5.32}$$

which is also the minimum distance.

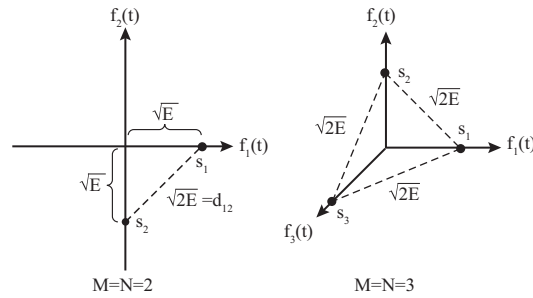


Figure 5.8 Orthogonal signals for  $M=N=2$  and  $M=N=3$

### Biorthogonal signals

A set of  $M$  biorthogonal signals can be constructed from  $(1/2)M$  orthogonal signals by simply including the negatives of the orthogonal signals. Thus, we require  $N = (1/2)M$  dimensions for the construction of a set of  $M$  biorthogonal signals.

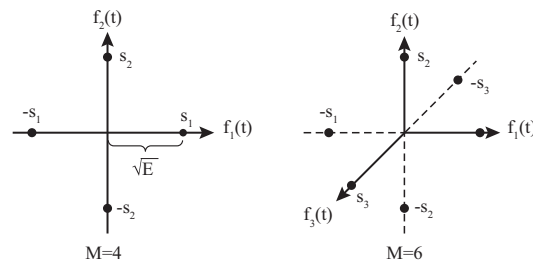


Figure 5.9 Signal space diagram for  $M = 4$  and  $M = 6$  biorthogonal signals

We note, that the correlation between any pair of waveforms is either  $\rho_r = -1$  or  $0$ . The corresponding distances are  $d = 2\sqrt{E}$  or  $d = \sqrt{2E}$ , with the latter being the minimum distance.

### Simplex signals

Suppose we have a set of  $M$  orthogonal waveforms  $\{s_m(t)\}$  or, equivalently, their vector representation  $\{s_m\}$ . Their mean is

$$\bar{s} = \frac{1}{M} \sum_{m=1}^M s_m \tag{5.33}$$

Now, let us construct another set of  $M$  signals by subtracting the mean from each of the  $M$  orthogonal signals. Thus



$$s'_m = s_m - \bar{s} \tag{5.34}$$

The effect of the subtraction is to translate the origin of the  $m$  orthogonal signals to the point  $\bar{s}$ .

The resulting signal waveforms are called *simplex signals* and have the following properties. First, the energy per waveform is

$$\begin{aligned} \|s'_m\|^2 &= \|s_m - \bar{s}\|^2 \\ &= E - \left(\frac{2}{M}\right)E + \left(\frac{1}{M}\right)E = E\left(1 - \frac{1}{M}\right) \end{aligned} \tag{5.35}$$

Second, the cross correlation of any pair of signals is

$$Re(\rho_{km}) = \frac{s'_m \cdot s'_k}{\|s'_m\| \|s'_k\|} = \frac{-1/M}{1-1/M} = -\frac{1}{M-1}, \text{ for all } m, n \tag{5.36}$$

Hence, the set of simplex waveforms is equally correlated and requires less energy, by the factor  $1 - 1/M$ , than the set of orthogonal waveforms. Since only the origin was translated, the distance between any pair of signal points is maintained at  $d = \sqrt{2E}$ , which is the same as the distance between any pair of orthogonal signals.

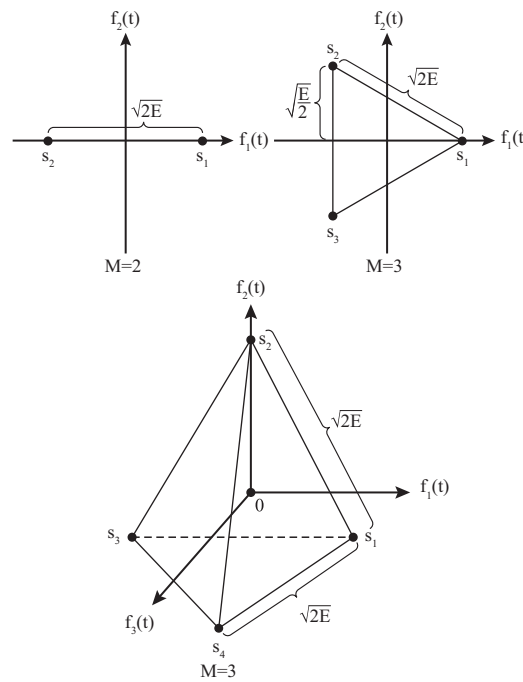


Figure 5.10 Signal space diagrams for M-ary simplex signals

### Signal waveforms from binary codes

A set of  $M$  signaling waveforms can be generated from a set of  $M$  binary code words of the form

$$C_m = [c_{m1}, c_{m2}, \dots, c_{mN}], \quad m=1, 2, \dots, M \tag{5.37}$$

where  $c_{mj} = 0$  or  $1$  for all  $m$  and  $j$ . Each component of a code word is mapped into an elementary binary PSK waveform as follows:

$$c_{mj} = 1 \Rightarrow s_{mj}(t) = \sqrt{\frac{2E_c}{T_c}} \cos 2\pi f_c t; \quad 0 \leq t \leq T_c \quad (5.38)$$

$$c_{mj} = 0 \Rightarrow s_{mj}(t) = -\sqrt{\frac{2E_c}{T_c}} \cos 2\pi f_c t; \quad 0 \leq t \leq T_c \quad (5.39)$$

where  $T_c = T/N$  and  $E_c = E/N$ . Thus, the  $M$  code words  $\{C_m\}$  are mapped into a set of  $M$  waveforms  $\{s_m\}$ . The waveforms can be represented in vector form as

$$s_m = [s_{m1}, s_{m2}, \dots, s_{mN}], \quad m=1, 2, \dots, M \quad (5.40)$$

where  $s_{mj} = \pm \sqrt{\frac{E}{N}}$  for all  $m$  and  $j$ .  $N$  is called the block length of the code, and it is also the dimension of the  $M$  waveforms.

We note that there are  $2^N$  possible waveforms that can be constructed from the  $2^N$  possible binary code words. We may select a subset of  $M < 2^N$  signal waveforms for transmission of information. We also observe that  $2^N$  possible signal points correspond to the vertices of an  $N$  – dimensional hypercube with its center at the origin. Figure 5.11 illustrates the signal points in  $N=2$  and 3 dimensions.

Each of the  $M$  waveforms has energy  $E$ . The cross correlation between any pair of waveforms depends on how we select the  $M$  waveforms from the  $2^N$  possible waveforms. Clearly, any adjacent signal points have a cross-correlation coefficient

$$\rho_r = \frac{E(1-2/N)}{E} = \frac{N-2}{N} \quad (5.41)$$

and a corresponding distance of

$$d^{(e)} = \sqrt{2E(1 - \rho_r)} = \sqrt{\frac{4E}{N}} \quad (5.42)$$

This concludes our discussion of memoryless modulation signals.

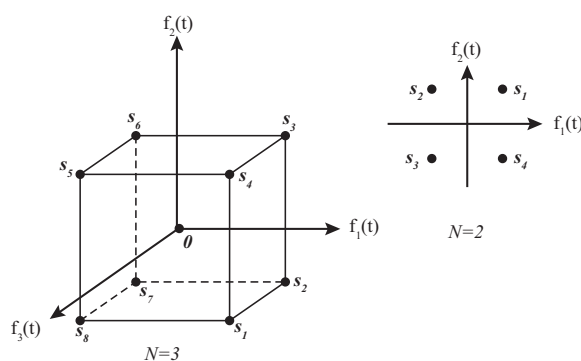


Figure 5.11 Signal space diagrams for signals generated from binary codes

### 5.3.2 Linear Modulation with Memory

In this section, we present some modulation signals in which there is dependence between the signals transmitted in successive symbol intervals. This signal dependence is usually introduced for the purpose of shaping the spectrum of the transmitted signal so that it matches the spectral characteristics of the channel.

We shall present examples of modulation signals with memory and characterize their memory in terms of Markov chains. We shall confine our treatment to baseband signals. The generalization to band-pass signals is relatively straightforward.

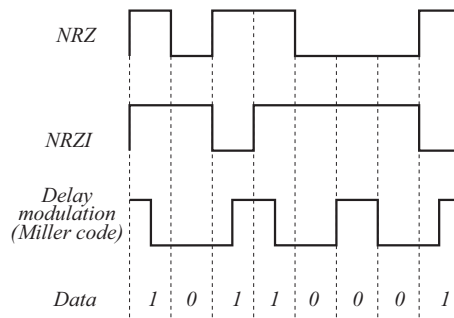


Figure 5.12 Examples of baseband signals

NRZ modulation is memoryless and is equivalent to a binary PAM or a binary PSK signal in a carrier-modulated system.

The NRZI signal is different from NRZ signal in that transitions from one amplitude level to another occur only when a 1 is transmitted. The amplitude level remains unchanged when zero is transmitted. NRZI is called differential encoding. The encoding operation is described mathematically by the relation

$$b_k = a_k \oplus b_{k-1} \tag{5.43}$$

where  $a_k$  is the input into the encoder and  $b_k$  is the output of the encoder. When  $b_k = 1$ , the transmitted waveform is a rectangular pulse of amplitude  $A$ , when  $b_k = 0$ , the transmitted waveform is a rectangular pulse of amplitude  $-A$ . Hence, the output of the decoder is mapped into one of two waveforms in exactly the same manner as for NRZ signal.

The differential encoding operation introduces memory in the signal. The combination of the encoder and the modulator operations may be represented by a state diagram (a Markov chain) as shown in Figure 5.13.

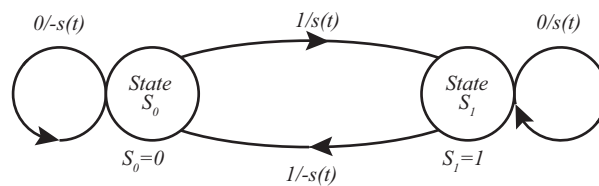


Figure 5.13 State diagram for the NRZI signal

The state diagram may be described by two transition matrices corresponding to the two possible input bits  $\{0,1\}$ . We note that when  $a_k = 0$ , the encoder stays in the same state. Hence, the state transition matrix for a zero is simply

$$T_1 = \begin{bmatrix} 1 & 0 \\ 0 & 1 \end{bmatrix} \tag{5.44}$$

where  $t_{ij} = 1$ , if  $a_k$  results in a transition from state  $i$  to state  $j$ ,  $i = 1,2$  and  $j = 1,2$ ; otherwise,  $t_{ij} = 0$ . Similarly, the state transition matrix for  $a_k = 1$  is

$$T_2 = \begin{bmatrix} 0 & 1 \\ 1 & 0 \end{bmatrix} \tag{5.45}$$

Thus, these two state transition matrices characterize the NRZI signal.

Another way to display the memory is by a trellis diagram. The trellis provides the same information concerning the signal dependence as the state diagram, but also depicts a time evolution of the state transitions.

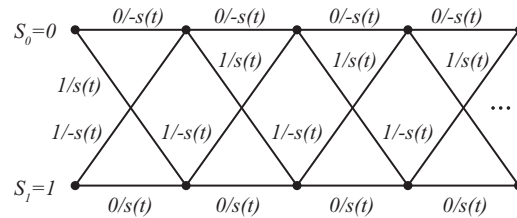


Figure 5.14 The trellis diagram for the NRZI signal

The signal generated by delay modulation also has memory. Delay modulation is equivalent to encoding the data sequence by a run-length-limited code called a Miller code and using NRZI to transmit the encoded data this type of modulation has been used extensively in binary PSK. The signal may be described by a state diagram that has four states as shown in Figure 5.15a). There are two elementary waveforms  $s_1(t)$  and  $s_2(t)$  and their negatives  $-s_1(t)$  and  $-s_2(t)$  which are used for transmitting the binary information. These waveforms are illustrated in Figure 5.15b). The mapping from bits to corresponding waveforms is illustrated in the state diagram. The state transition matrices that characterize the memory of this encoding and modulation method are easily obtained from the state diagram in Figure 5.15. When  $a_k = 0$ , we have

$$T_1 = \begin{bmatrix} 0 & 0 & 0 & 1 \\ 0 & 0 & 0 & 1 \\ 1 & 0 & 0 & 0 \\ 1 & 0 & 0 & 0 \end{bmatrix} \tag{5.46}$$

and when  $a_k = 1$ , the transition matrix is

$$T_2 = \begin{bmatrix} 0 & 1 & 0 & 0 \\ 0 & 0 & 1 & 0 \\ 0 & 1 & 0 & 0 \\ 0 & 0 & 1 & 0 \end{bmatrix} \tag{5.47}$$

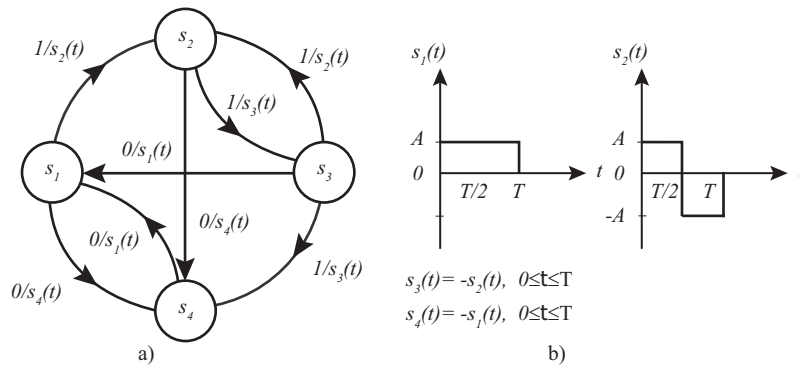


Figure 5.15 a) State diagram and basic waveforms b) for delay modulated (Miller-encoded) signal

Modulation techniques with memory such as NRZI coding are generally characterized by a  $K$ -state Markov chain with *stationary state probabilities*  $\{p_i = 1, 2, \dots, K\}$  and *transition probabilities*  $\{p_{ij}; i, j = 1, 2, \dots, K\}$ . Thus, the transition probability  $p_{ij}$  denotes the probability that signal waveform  $s_j(t)$  is transmitted in a given signaling interval after the transmission of the signal waveform  $s_i(t)$  in the previous signaling interval. The transition probabilities may be arranged in matrix form as

$$T_2 = \begin{bmatrix} p_{11} & p_{12} & \cdot & p_{1K} \\ p_{21} & p_{22} & \cdot & p_{2K} \\ \cdot & \cdot & \cdot & \cdot \\ p_{K1} & p_{K2} & \cdot & p_{KK} \end{bmatrix} \quad (5.48)$$

where  $P$  is called the *transition probability matrix*.

The transition probability matrix is easily obtained from the transition matrices  $\{T_i\}$  and the corresponding probabilities of occurrence of the input bits (or, equivalently, the stationary state transition probabilities  $\{p_i\}$ ). The general relationship may be expressed as

$$P = \sum_{i=1}^2 q_i T_i \quad (5.49)$$

where  $q_1 = P(a_k = 0)$  and  $q_2 = P(a_k = 1)$ .

For the NRZI signal with equal state probabilities  $p_1 = p_2 = \frac{1}{2}$  and transition matrices given by Equations 5.44 and 5.45, the transition probability matrix is

$$P = \begin{bmatrix} 1/2 & 1/2 \\ 1/2 & 1/2 \end{bmatrix} \quad (5.50)$$

Similarly, the transition probability matrix for the Miller-coded signal with equally likely symbols ( $q_1 = q_2 = 1/2$  or, equivalently,  $p_1 = p_2 = p_3 = p_4 = 1/4$ ) is

$$P = \begin{bmatrix} 0 & 1/2 & 0 & 1/2 \\ 0 & 0 & 1/2 & 1/2 \\ 1/2 & 1/2 & 0 & 0 \\ 1/2 & 0 & 1/2 & 0 \end{bmatrix} \quad (5.51)$$

The transition probability matrix is useful in the determination of the spectral characteristics of digital modulation techniques with memory, as we shall observe in Section 5.4.

### 5.3.3 Non-Linear Modulation Methods with Memory

#### **Continuous-phase FSK (CPFSK)**

To avoid the use of signals having large spectral side lobes, the information-bearing signal frequency modulates a single carrier whose frequency is changed continuously (CPFSK). This type of FSK signal has memory because the phase of the carrier is constrained to be continuous.

In order to represent a CPFSK signal, we begin with a PAM signal

$$d(t) = \sum_n I_n g(t - nT) \quad (5.52)$$

where  $\{I_n\}$  denotes the sequence of amplitudes obtained by mapping  $k$ -bit blocks of binary digits from the information sequence  $\{a_n\}$  into the amplitude levels  $\pm 1, \pm 3, \dots, \pm(M-1)$  and  $g(t)$  is a

rectangular pulse of amplitude  $1/2$  and duration  $T$  seconds. The signal  $d(t)$  is used to frequency-modulate the carrier. Consequently, the equivalent low-pass waveform  $v(t)$  is expressed as

$$v(t) = \sqrt{\frac{2E}{T}} \exp\{j[4\pi T f_d \int_{-\infty}^t d(\tau) d\tau + \phi_0]\} \quad (5.53)$$

where  $f_d$  is the peak frequency deviation and  $\phi_0$  is the initial phase of the carrier. The carrier-modulated signal corresponding to Equation 4.53 may be expressed as

$$v(t) = \sqrt{\frac{2E}{T}} \cos[2\pi T f_c t + \phi(t; I) + \phi_0] \quad (5.54)$$

where  $\phi(t; I)$  represents the time-varying phase of the carrier, which is defined as

$$\phi(t; I) = 4\pi T f_d \int_{-\infty}^t d(\tau) d\tau = 4\pi T f_d \int_{-\infty}^t \sum_n [I_n g(t - nT)] d\tau \quad (5.55)$$

Note that, although  $d(t)$  contains discontinuities, the integral of  $d(t)$  is continuous. Hence, we have a continuous-phase signal. The phase of the carrier in the interval  $nT \leq t \leq (n+1)T$  is determined by integrating Equation 5.55. Thus,

$$\phi(t; I) = 2\pi T f_d \sum_{k=-\infty}^{n-1} I_k + 2\pi T f_d (t - nT) I_n = \theta_n + 2\pi h I_n g(t - nT) \quad (5.56)$$

where  $h$ ,  $\theta_n$  and  $g_n$  are defined as

$$h = 2T f_d \quad (5.57)$$

$$\theta_n = \pi h \sum_{k=-\infty}^{n-1} I_k \quad (5.58)$$

$$q(t) = \begin{cases} 0, & (t < 0) \\ t/2T, & (0 \leq t \leq T) \\ 1/2, & (t > T) \end{cases} \quad (5.59)$$

We observe that  $\theta_n$  represents the accumulation (memory) of all symbols up to time  $(n-1)T$ . The parameter  $h$  is called the modulation index.

### **Continuous-phase modulation (CPM)**

When expressed in the form Equation 4.56, CPFSK becomes a special case of a general phase of continuous-phase modulated (CPM) signal in which the carrier phase is

$$\phi(t; I) = 2\pi \sum_{k=-\infty}^{n-1} I_k h_k g(t - kT), \quad nT \leq t \leq (n+1)T \quad (5.60)$$

where  $\{I_k\}$  is the sequence of  $M$ -ary information symbols selected from the  $\{\pm 1, \pm 3, \dots, \pm(M-1)\}$ ,  $\{h_k\}$  is a sequence of modulation indices, and  $q(t)$  is some normalized waveform shape.

When  $h_k = h$  for all  $k$ , the modulation index is fixed for all symbols. When the modulation index varies from one symbol to another, the CPM signal is called *multi-h*. In such a case, the  $\{h_k\}$  are made to vary in a cyclic manner through a set of indices.

The waveform  $q(t)$  may be represented in general as the integral of some pulse  $g(t)$ , i.e.,

$$g(t) = \int_0^t g(\tau) d\tau \quad (5.61)$$

If  $g(t) = 0$  for  $t > T$ , the CPM signal is called full response CPM. If for  $t > T$ , the modulated signal is called *partial response* CPM. Figure 5.16 illustrates several pulse shapes for  $g(t)$ , and corresponding  $q(t)$ . It is apparent that an infinite variety of CPM signals can be generated by choosing different pulse shapes  $g(t)$  and by varying the modulation index  $h$  and the alphabet size  $M$ .

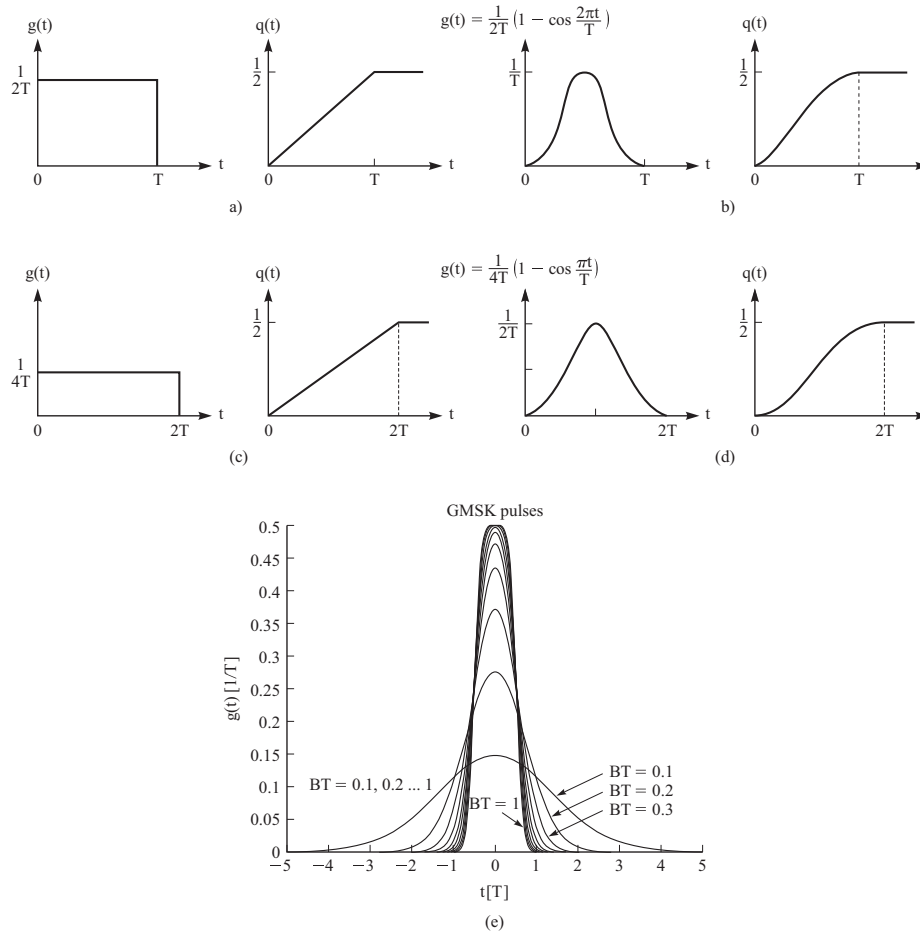


Figure 5.16 Pulse shapes for full-response CPM (a, b) and partial-response CPM (c, d), and GMSK (e)

We note that the CPM signal has memory that is introduced through the phase continuity. For  $L > 1$ , additional memory is introduced in the CPM signal by the pulse  $g(t)$ .

Three popular pulse shapes are given:

$$\text{LREC } g(t) = \begin{cases} \frac{1}{2LT}, & (0 \leq t \leq LT) \\ 0, & \text{otherwise} \end{cases}$$

$$\text{LRC } g(t) = \begin{cases} \frac{1}{2LT} (1 - \cos \frac{2\pi t}{LT}), & (0 \leq t \leq LT) \\ 0, & \text{otherwise} \end{cases}$$

$$\text{LRC } g(t) = \left\{ Q \left[ \frac{2\pi B (t - \frac{T}{2})}{(\ln 2)^{\frac{1}{2}}} \right] - Q \left[ \frac{2\pi B (t + \frac{T}{2})}{(\ln 2)^{\frac{1}{2}}} \right] \right\}$$

$$Q(x) = \int_x^{\infty} \frac{1}{\sqrt{2\pi}} e^{-\frac{x^2}{2}} dt$$



LREC denotes a rectangular pulse duration  $LT$ , where  $L$  is a positive integer. In this case,  $L = 1$  results in a CPSK signal, with the pulses as shown in Figure 5.16a. The LREC pulse for  $L = 2$  is shown in Figure 5.16c. LRC denotes a raised cosine pulse of duration  $LT$ . The LRC pulses corresponding to  $L = 1$  and  $L = 2$  are shown in Figure 5.16b and d, respectively. The third pulse is called a Gaussian minimum-shift keying (GMSK) pulse with bandwidth parameter  $B$ , which represents the  $-3dB$  bandwidth of the Gaussian pulse. Figure 5.16e illustrates a set of GMSK pulses with time-bandwidth products  $BT$  ranging from 0.1 to 1. We observe that the pulse duration increases as the bandwidth of the pulse decreases, as expected. In practical applications, the pulse is usually truncated to some specific fixed duration. GMSK with  $BT = 0.3$  is used in the European digital cellular communication system, called GSM. From Figure 5.16e we observe that when  $BT = 0.3$ , the GMSK pulse may be truncated at  $|t| = 1.5T$  with a relatively small error incurred for  $T > 1.5T$ .

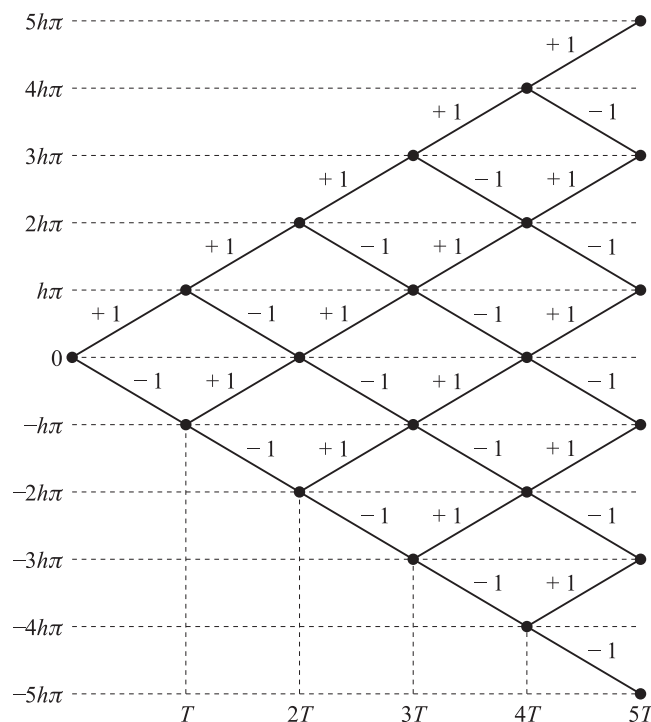


Figure 5.17 Phase trajectory for binary CPFSK

It is instructive to sketch the set of phase trajectories  $\phi(t; I)$  generated by all possible values of the information sequence  $\{I_n\}$ . For example, in the case of CPFSK with binary symbols  $I_n = \pm 1$ , the set of phase trajectories beginning at time  $t = 0$  is shown in Figure 5.17. For comparison, the phase trajectories for quaternary CPFSK are illustrated in Figure 5.19.

These phase diagrams are called *phase trees*. We observe that the phase trees for CPFSK are piecewise linear as a consequence of the fact that the pulse  $g(t)$  is rectangular. Smoother phase trajectories and phase trees are obtained by using pulses that do not contain discontinuities, such as the pulse of raised cosine pulses. For example, a phase trajectory generated by the sequence  $(1, -1, -1, -1, 1, 1, -1, 1)$  for a partial response, raised cosine pulse of length  $3T$  is illustrated in Figure 5.18. For comparison, the corresponding phase trajectory generated by CPFSK is also shown.

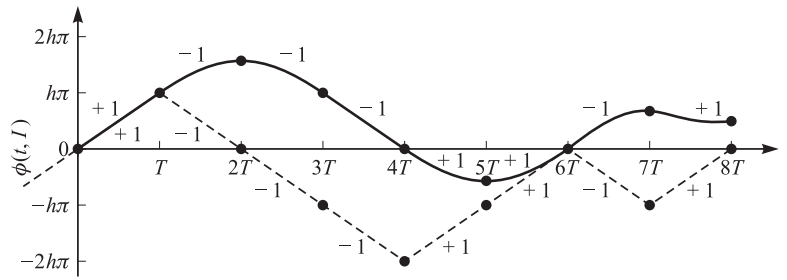


Figure 5.18 Phase trajectories for binary CPFSK (dashed) and binary, partial-response CPM based on raised cosine pulse of length  $3T$  (solid) [Source: Sundberg (1986), ©1986 IEEE]

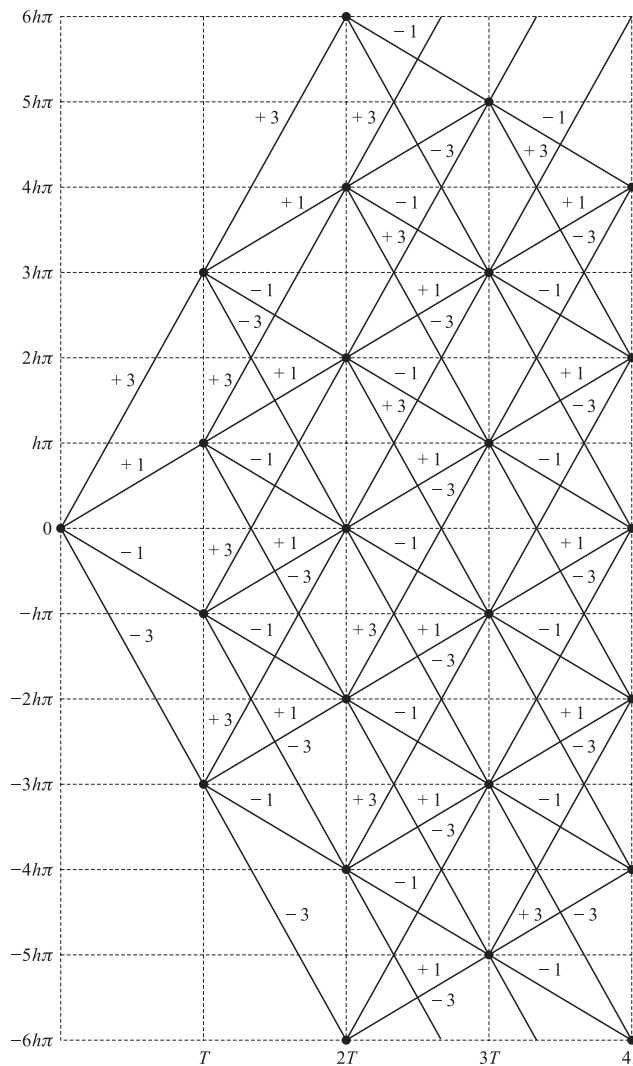


Figure 5.19 Phase trajectory for quaternary CPFSK

**Minimum-shift keying (MSK)**

MSK is a special form of CPFSK (and, therefore, CPM) in which the modulation index  $h = \frac{1}{2}$ . The phase of the carrier in the interval  $nT \leq t \leq (n + 1)T$  is

$$\phi(t; I) = \frac{1}{2} \pi \sum_{k=-\infty}^{n-1} I_k + \pi I_n g(t - nT) I_n = \theta_n + \frac{1}{2} \pi I_n \left( \frac{t - nT}{T} \right), nT \leq t \leq (n + 1)T \quad (5.62)$$

and the modulated carrier signal is

$$s(t) = A \cos \left[ 2\pi f_c t + \theta_n + \frac{1}{2} \pi I_n \left( \frac{t-nT}{T} \right) \right] = A \cos \left[ 2\pi \left( f_c + \frac{1}{4T} I_n \right) t - \frac{1}{2} n\pi I_n + \theta_n \right] \quad (5.63)$$

The expression 5.63 indicates that the binary CPFSK signal can be expressed as a sinusoid having one of two possible frequencies in the interval  $nT \leq t \leq (n+1)T$ . If we denote these frequencies as

$$f_1 = f_c - \frac{1}{4T}, \quad f_2 = f_c + \frac{1}{4T} \quad (5.64)$$

Then the binary CPFSK signal given by Equation 5.63 may be written in the form

$$s(t) = A \cos \left[ 2\pi f_i t + \theta_n + \frac{1}{2} n\pi (-1)^{i-1} \right], \quad i = 1, 2 \quad (5.65)$$

The frequency separation  $\Delta f = f_2 - f_1$ . Recall that  $\Delta f = \frac{1}{2} T$  is the minimum frequency separation that is necessary to ensure the orthogonality of the signals  $s_1(t)$  and  $s_2(t)$  over a signalling interval of length  $T$ . This explains why binary CPFSK with  $h = \frac{1}{2}$  is called **minimum-shift keying (MSK)**.

**Signal space diagrams for CPM.** In general, continuous-phase signals cannot be represented by discrete points in signal space as in the case of PAM, PSK, and QAM, because the phase of the carrier is time-variant. Instead, a continuous-phase signal is described by the various paths or trajectories from one phase state to another. For a constant-amplitude CPM signal, the various trajectories form a circle. For example, Figure 5.20 illustrates the signal space (phase trajectory) diagram for CPFSK signals with  $h = \frac{1}{4}$ ,  $h = \frac{1}{3}$ ,  $h = \frac{1}{2}$ , and  $h = \frac{2}{3}$ . The beginning and ending points of these phase trajectories are marked in the figure by dots. Note that the length of the phase trajectory increases with an increase in  $h$ . An increase in  $h$  also results in an increase of the signal bandwidth, as demonstrated in the following section.

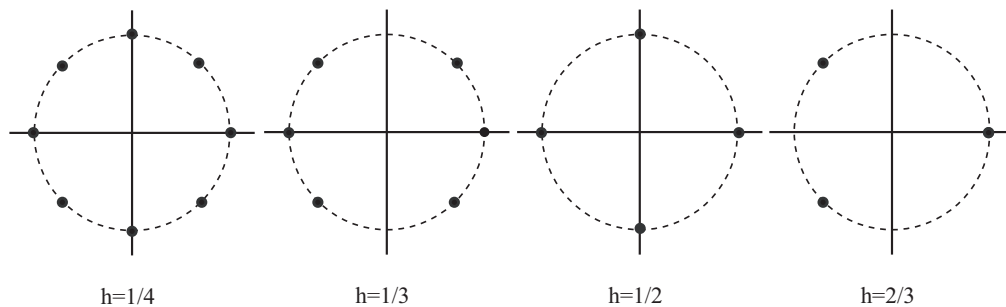


Figure 5.20 Signal space diagram for CPFSK

**A linear representation of CPM.** As described above, CPM is a non-linear modulation technique with memory. However, CPM may also be represented as a linear superposition of signal waveforms.

**Multiamplitude CPM.** Multiamplitude CPM is a generalization of ordinary CPM in which the signal amplitude is allowed to vary over a set of amplitude values while the phase of the signal is constrained to be continuous.

## 5.4 SPECTRAL CHARACTERISTIC OF DIGITALLY MODULATED SIGNALS

In most digital communication systems, the available channel bandwidth is limited. Consequently, the system designer must consider the constraints imposed by the channel bandwidth limitation in the selection of the modulation technique used to transmit the information. For this reason, it is important for us to determine the spectral content of the digitally modulated signals.

Since the information sequence is random, a digitally modulated signal is a stochastic process. We are interested in determining the power density spectrum of such a process. From the power density spectrum we can determine the channel bandwidth required to transmit the information-bearing signal.

### 5.4.1 Power Spectra of Linearly Modulated Signals

Beginning with the form

$$s(t) = \text{Re}[v(t)e^{j2\pi f_c t}]$$

which relates the band-pass signal  $s(t)$  to the equivalent low-pass signal  $v(t)$ , we may express the autocorrelation function of  $s(t)$  as

$$\phi_{ss}(\tau) = \text{Re}[\phi_{vv}(\tau)e^{j2\pi f_c \tau}] \quad (5.66)$$

where  $\phi_{vv}(\tau)$  is the autocorrelation function of the equivalent low-pass signal  $v(t)$ .

The Fourier transform of Equation 5.66 yields the desired expression for the power density spectrum in the form

$$\Phi_{ss}(f) = \frac{1}{2}[\Phi_{vv}(f - f_c) + \Phi_{vv}(-f - f_c)] \quad (5.67)$$

Where  $\Phi_{vv}(f)$  is the power density spectrum of  $v(t)$ .

First we consider the linear digital modulation method for which  $v(t)$  is represented in the general form

$$v(t) = \sum_{n=-\infty}^{\infty} I_n g(t - nT) \quad (5.68)$$

where the transmission rate is  $1/T = R/k$  symbols/s and  $\{I_n\}$  represents the sequence of symbols that results from mapping  $k$ -bit blocks into corresponding signal points selected from the appropriate signal space diagram. Observe that in PAM, the sequence  $\{I_n\}$  is real and corresponds to the amplitude values of the transmitted signal, but in PSK, QAM, and combined PAM-PSK, the sequence  $\{I_n\}$  is complex-valued, since the signal points have a two-dimensional representation.

The average power density spectrum of  $v(t)$  is

$$\Phi_{vv}(f) = \frac{1}{2}|G(f)|^2 \Phi_{ii}(f) \quad (5.69)$$

where  $G(f)$  is the Fourier transform of  $g(t)$ , and  $\Phi_{ii}(f)$  denotes the power density spectrum of the information sequence, defined as

$$\Phi_{ii}(f) = \sum_{m=-\infty}^{\infty} \Phi_{ii}(m) e^{-j2\pi f m T} \quad (5.70)$$

The result 5.69 illustrates the dependence of the power density spectrum of  $v(t)$  on the spectral characteristics of the pulse  $g(t)$  and the information sequence  $\{I_n\}$ . That is, the spectral characteristics of  $v(t)$  can be controlled by design of the pulse shape  $g(t)$  and by design of the correlation characteristics of the information sequence.

The desired power density spectrum of  $v(t)$  when the sequence of information symbols is uncorrelated is in the form

$$\Phi_{vv}(f) = \frac{\sigma_i^2}{T} |G(f)|^2 + \frac{\mu_i^2}{T^2} \sum_{m=-\infty}^{\infty} \left| G\left(\frac{m}{T}\right) \right|^2 \delta\left(f - \frac{m}{T}\right) \quad (5.71)$$

Where  $\sigma_i^2$  denotes the variance of an information symbol and  $\mu_i$  denotes the mean.

The expression 5.71 for the power density spectrum is purposely separated into two terms to emphasize the two different types of spectral components. The first term is the continuous spectrum, and its shape depends only on the spectral characteristic of the signal pulse  $g(t)$ . The second term consists of discrete frequency components spaced  $1/T$  apart in frequency. Each spectral line has a power that is proportional to  $\left| G\left(\frac{m}{T}\right) \right|^2$  evaluated at  $f = m/T$ . Note that the discrete frequency components vanish when the information symbols have zero mean, i.e.,  $\mu_i = 0$ . This condition is usually desirable for the digital modulation techniques under consideration, and it is satisfied when the information symbols are equally likely and symmetrically positioned in the complex plane. Thus, the system designer can control proper selection of the characteristics of the information sequence to be transmitted.

#### 5.4.2 Power Spectra of CPFSK and CPM Signals

The power density spectrum of CPFSK for  $M = 2, 4,$  and  $8$  is plotted in Figures 5.21 to 5.23 as a function of the normalized frequency  $fT$ , with the modulation index  $h = 2 f_d T$  as a parameter. Note that only one-half of the bandwidth occupancy is shown in Figure 5.21.

The origin corresponds to the carrier  $f_c$ . The graphs illustrate that the spectrum of CPFSK is relatively smooth and well confined for  $h < 1$ . As  $h$  approaches unity, the spectra become very peaked, and for  $h = 1$  when  $|\Phi| = 1$ , we find that impulses occur at  $M$  frequencies. When  $h > 1$ , the spectrum becomes much broader. In communication systems where CPFSK is used, the modulation index is designed to conserve bandwidth, so that  $h < 1$ .

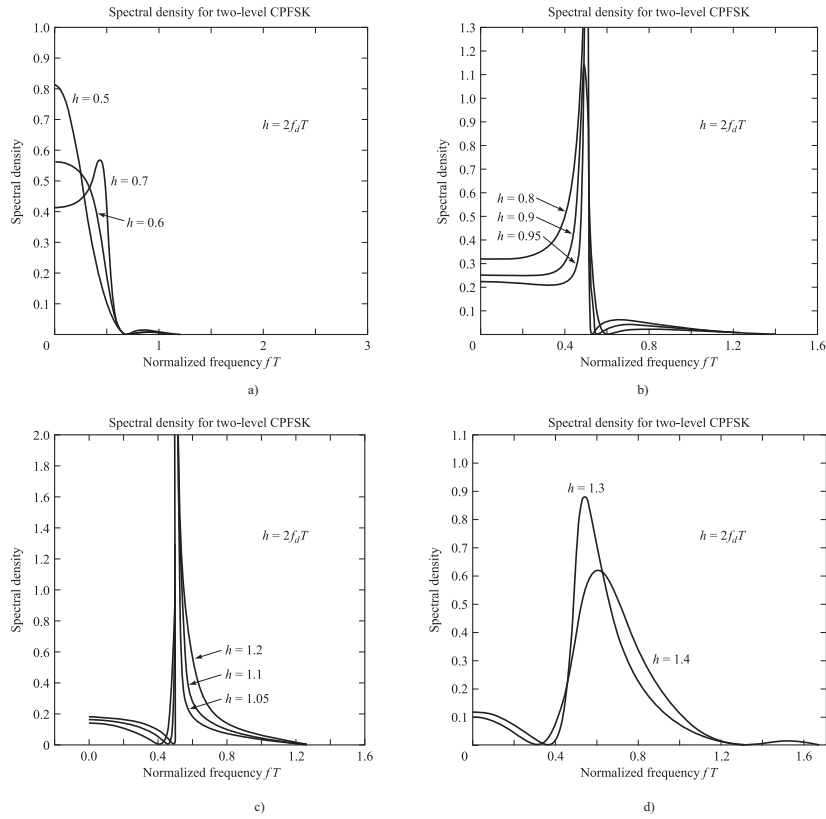


Figure 5.21 Power spectral density of binary CPFSK

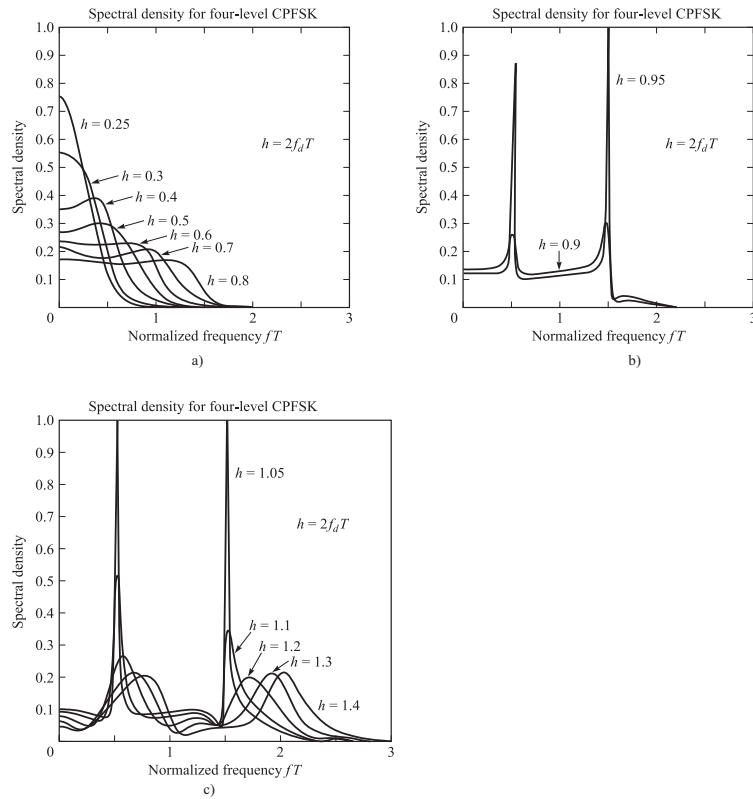


Figure 5.22 Power spectral density of quaternary CPFSK

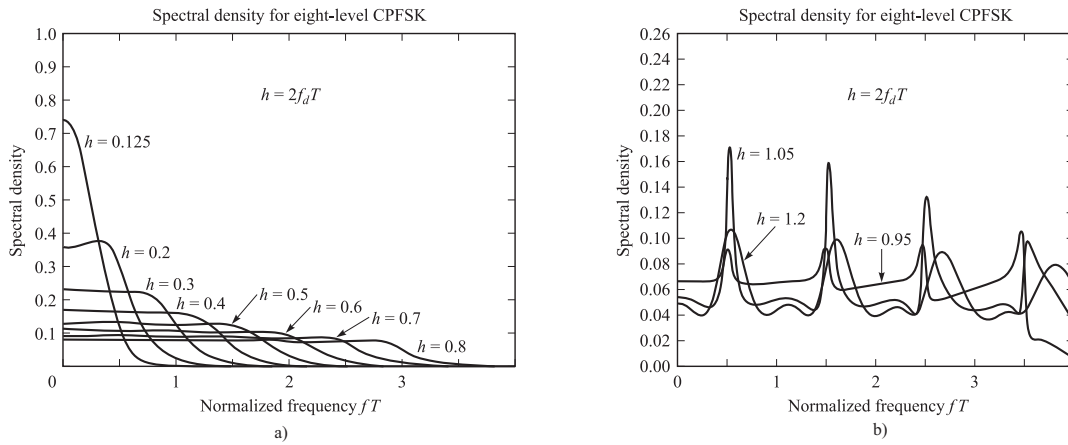


Figure 5.23 Power spectral density of octal CPFSK

In general, the bandwidth occupancy of CPM depends on the choice of the modulation index  $h$ , the pulse shape  $g(t)$ , and the number of signals  $M$ . As we have observed for CPFSK, small values of  $h$  result in CPM signals with relatively small bandwidth occupancy, while large values of  $h$  result in signals with large bandwidth occupancy. This is also the case for the more general CPM signals.

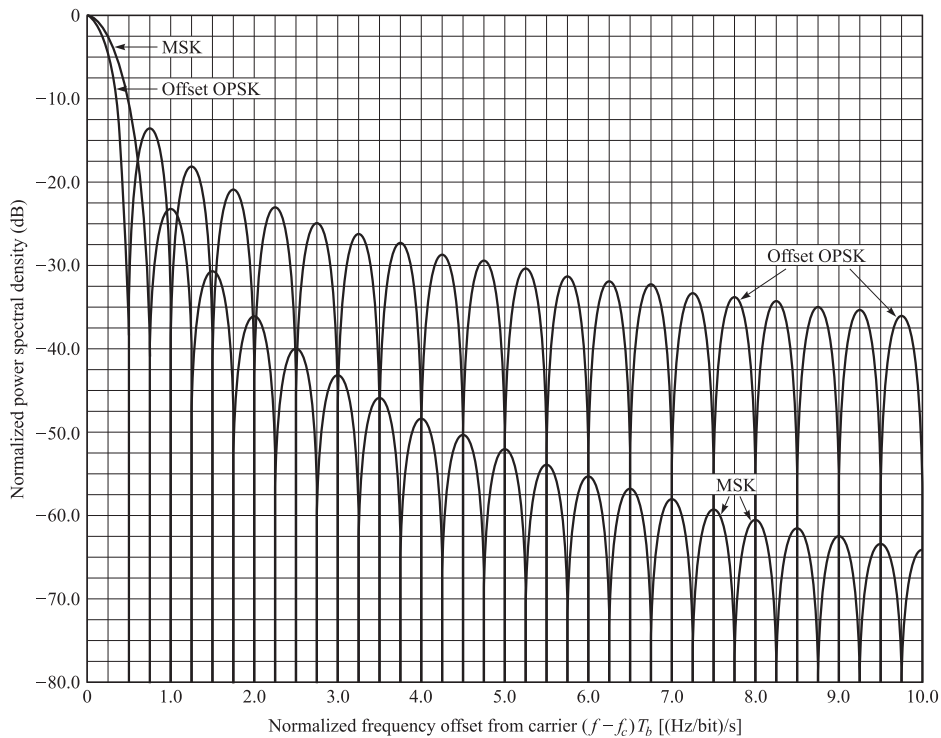


Figure 5.24 Power spectral density of MSK and QPSK. [Source: Gronemeyer and McBride (1976);© IEEE.]



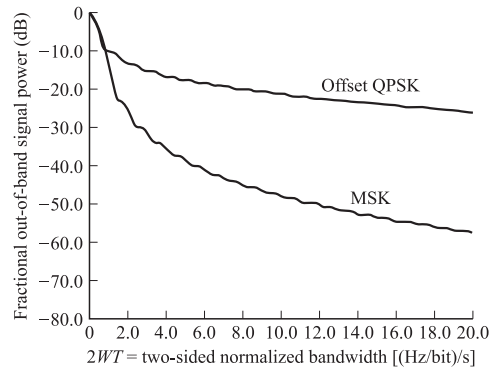


Figure 5.25 Fractional out-of-band power (normalized two-sided bandwidth =  $2WT$ ). [Source: Gronemeyer and McBride ;© IEEE.]

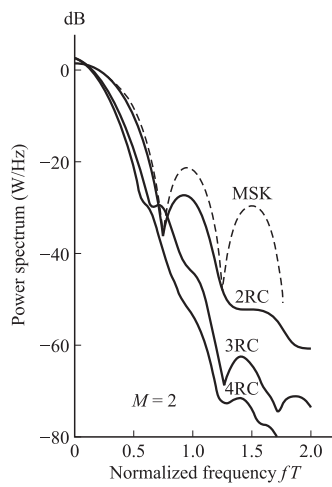


Figure 5.26 Power spectral density for binary CPM with  $h = 1/2$  and different pulse shapes. [Source: Aulin et al. (1981);© IEEE.]

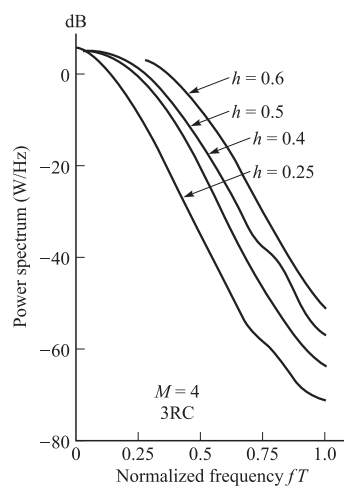


Figure 5.27 Power spectral density for  $M = 4$  CPM with 3RC and different modulation indices. [Source: Aulin et al. (1981);© IEEE.]

### 5.4.3 Solved Problems

#### Problem 1

To illustrate the spectral shaping resulting from  $g(t)$ , consider the rectangular pulse shown in Figure a).

*Solution*

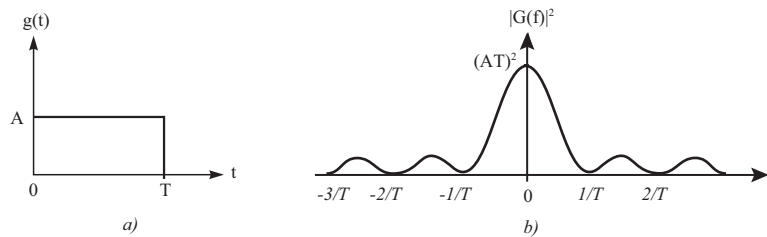
The Fourier transform of  $g(t)$  is

$$G(f) = (AT)^2 \frac{\sin \pi f T}{\pi f T} e^{-j\pi f T}$$

Hence

$$|G(f)|^2 = (AT)^2 \left( \frac{\sin \pi f T}{\pi f T} \right)^2$$

This spectrum is illustrated in Figure b).



Note that it contains zeros at multiples of  $1/T$  in frequency and that it decays inversely as the square of the frequency variable. As a consequence of the spectral zeros in  $G(f)$ , all but one of the discrete spectral components in Equation 5.71 vanish. Thus upon substitution for  $|G(f)|^2$  reduces to

$$\Phi_{vv}(f) = \sigma_i^2 A^2 T \left( \frac{\sin \pi f T}{\pi f T} \right)^2 + A^2 \mu_i^2 \delta(f) \quad (5.72)$$

#### Problem 2

As a second illustration of the spectral shaping resulting from  $g(t)$ , we consider the raised cosine pulse

$$g(t) = \frac{A}{2} \left[ 1 + \cos \frac{2\pi}{T} \left( t - \frac{T}{2} \right) \right], 0 \leq t \leq T$$

*Solution*

This pulse is graphically illustrated in Figure 2. Its Fourier transform is easily derived, and it may be expressed in the form

$$G(f) = \frac{AT}{2} \frac{\sin \pi f T}{\pi f T (1 - f^2 T^2)} e^{-j\pi f T}$$

Consequently, all the discrete spectral components in Equation 5.71, except the one at  $f = 0$  and  $= \pm 1/T$ , vanish. When compared with the spectrum of the rectangular pulse, the spectrum of the raised cosine pulse has a broader main lobe but the tails decay inversely as  $f$ .

**Problem 3**

To illustrate that spectral shaping can also be accomplished by operations performed on the input information sequence, we consider a binary sequence  $\{b_n\}$  from which we form the symbols

$$I_n = b_n + b_{n-1}$$

The  $\{b_n\}$  are assumed to be uncorrelated random variables, each having zero mean and unit variance. Then the autocorrelation function of the sequence  $\{I_n\}$  is

$$\phi_{ii}(m) = E(I_n I_{n+m}) = \begin{cases} 2 & (m = 0) \\ 1 & (m = \pm 1) \\ 0 & (\text{otherwise}) \end{cases}$$

Hence, the power density spectrum of the input sequence is

$$\phi_{ii}(f) = 2(1 + \cos 2\pi fT) = 4\cos^2 \pi fT$$

and the corresponding power density spectrum for the (low-pass) modulated signal is

$$\Phi_{vv}(f) = \frac{4}{T} |G(f)|^2 \cos^2 \pi fT$$

**Problem 4**

Consider an equivalent low-pass digitally modulated signal of the form

$$u(t) = \sum_n a_n g(t - 2nT) - j b_n g(t - 2nT - T)$$

where  $\{a_n\}$  and  $\{b_n\}$  are two sequences of statistically independent binary digits and  $g(t)$  is a sinusoidal pulse defined as

$$g(t) = \begin{cases} \sin\left(\frac{\pi t}{2T}\right), & 0 < t < 2T \\ 0, & \text{otherwise} \end{cases}$$

This type of signal is viewed as a four-phase PSK signal in which the pulse shape is one-half cycle of a sinusoid. Each of the information sequences  $\{a_n\}$  and  $\{b_n\}$  is transmitted at rate of  $\frac{1}{2}T$  bits/s and, hence, the combined transmission rate is  $\frac{1}{T}$  bits/s. The two sequences are staggered in time by  $T$  seconds in transmission. Consequently, the signal  $u(t)$  is called staggered *four-phase PSK*.

- a) Show that the envelope  $|u(t)|$  is a constant, independent of the information  $a_n$  on the in-phase component and information  $b_n$  on the quadrature component. In other words, the amplitude of the carries used in transmitting the signal is constant.
- b) Determine the power density spectrum of  $u(t)$ .
- c) Compare the power density spectrum obtained from (b) with the power density spectrum of the MSK signal. What conclusion can you draw from this comparison?

*Solution*

- a) Since the signaling rate is  $\frac{1}{2}T$  for each sequence and since  $g(t)$  has duration  $2T$ , for any time instant only  $g(t - 2nT)$  and  $g(t - 2nT - T)$  or  $g(t - 2nT + T)$  will contribute to  $u(t)$ . Hence, for  $2nT \leq t \leq 2nT + T$

$$\begin{aligned} |u(t)|^2 &= |a_n g(t - nT) - j b_n g(t - nT + T)|^2 \\ &= a_n^2 g^2(t - nT) + b_n^2 g^2(t - nT + T) \\ &= g^2(t - nT) + g^2(t - nT + T) = \sin^2 \frac{2\pi t}{2T} + \sin^2 \frac{2\pi(t + T)}{2T} \\ &= \sin^2 \frac{2\pi t}{2T} + \cos^2 \frac{2\pi t}{2T} = 1, \quad \forall t \end{aligned}$$

- b) The power density spectrum is:

$$\Phi_{vv}(f) = \frac{1}{T} |G(f)|^2$$

Where  $G(f) = \int_{-\infty}^{\infty} g(t) e^{-j2\pi f t} dt = \int_0^{2T} \sin \frac{\pi t}{2T} e^{-j2\pi f t} dt$ . By using trigonometric identity  $\sin x = \frac{e^{jx} - e^{-jx}}{2j}$  it is easily shown that:

$$G(f) = \frac{4T}{\pi} \frac{\cos 2\pi T f}{1 - 16T^2 f^2} e^{-j2\pi f T}$$

Hence

$$\begin{aligned} G(f) &= \left(\frac{4T}{\pi}\right)^2 \frac{\cos^2 2\pi T f}{(1 - 16T^2 f^2)^2} \\ G(f) &= \left(\frac{4T}{\pi}\right)^2 \frac{\cos^2 2\pi T f}{(1 - 16T^2 f^2)^2} \\ \Phi_{vv}(f) &= \frac{1}{T} \left(\frac{4T}{\pi}\right)^2 \frac{\cos^2 2\pi T f}{(1 - 16T^2 f^2)^2} = \frac{16T}{\pi^2} \frac{\cos^2 2\pi T f}{(1 - 16T^2 f^2)^2} \end{aligned}$$

- c) The above power density spectrum is identical to that for the MSK signal. Therefore, the MSK signal can be generated as a staggered four phase PSK signal with a half-period sinusoidal pulse for  $g(t)$

### **Problem 5**

The low-pass equivalent representation of PAM signal is

$$u(t) = \sum_n I_n g(t - nT)$$

Suppose  $g(t)$  is a rectangular pulse and

$$I_n = a_n - a_{n-2}$$

where  $\{a_n\}$  is a sequence of uncorrelated binary-valued (1,-1) random variables that occur with equal probability.

- Determine the autocorrelation function of the sequence  $\{I_n\}$ .
- Determine the power density spectrum of  $u(t)$ .
- Repeat (b) if the possible values of the  $a_n$  are (0,1).

*Solution*

a)  $I_n = a_n - a_{n-2}$  with the sequence  $\{a_n\}$  being uncorrelated random variables (i.e  $E(a_{n+m}a_n) = \delta(m)$ ). Hence

$$\begin{aligned}\Phi_{ii}(m) &= E[I_{n+m}I_n] = E[(a_{n+m}a_{n+m-2})(a_n a_{n-2})] \\ &= 2\delta(m) - \delta(m-2) - \delta(m+2) \\ &= \begin{cases} 2, & m = 0 \\ -1, & m = \pm 2 \\ 0, & \text{otherwise} \end{cases}\end{aligned}$$

b)  $\Phi_{uu}(f) = \frac{1}{T} |G(f)|^2 \Phi_{ii}(f)$  where:

$$\Phi_{ii}(f) = \sum_{m=-\infty}^{\infty} \phi_{ii}(m) e^{-j2\pi f m T} = 2 - e^{j4\pi f T} e^{-j4\pi f T} = 2[1 - \cos 4\pi f T]$$

And

$$|G(f)|^2 = (AT)^2 \left( \frac{\sin \pi f T}{\pi f T} \right)^2$$

Therefore:

$$\Phi_{uu}(f) = 4A^2 T \left( \frac{\sin \pi f T}{\pi f T} \right)^2 \sin^2 2\pi f T$$

c) If  $\{a_n\}$  takes the values (0,1) with equal probability then  $E(a_n) = 1/2$  and  $E(a_{n+m}a_n) =$

$$\begin{cases} \frac{1}{4}, & m = n \\ \frac{1}{2}, & m \neq n \end{cases} = \frac{[1+\delta(m)]}{4}, \text{ then:}$$

$$\begin{aligned}\phi_{ii}(f) &= E[I_{n+m}I_n] = 2\phi_{aa}(0) - \phi_{aa}(2) - \phi_{aa}(-2) \\ &= \frac{1}{4} [2\delta(m) - \delta(m-2) - \delta(m+2)]\end{aligned}$$

And

$$\Phi_{ii}(f) = \sum_{m=-\infty}^{\infty} \phi_{ii}(m) e^{-j2\pi f m T} = \sin^2 2\pi f T$$

$$\Phi_{uu}(f) = A^2 T \left( \frac{\sin \pi f T}{\pi f T} \right)^2 \sin^2 2\pi f T$$

Thus, we obtain the same results as in (b), but the magnitude of the various quantities is reduced by a factor of 4.

## 5.5 SUMMARY

- Pulse-amplitude modulation results when the amplitude of each carrier pulse is proportional to the value of the message signal at each sampling instant. Pulse-amplitude modulation is essentially a sample-and-hold operation. Demodulation of PAM is accomplished by lowpass filtering.
- Pulse-width modulation results when the width of each carrier pulse is proportional to the value of the message signal at each sampling instant. Demodulation of PWM is also accomplished by lowpass filtering.
- Pulse-position modulation results when the position of each carrier pulse, as measured by the displacement of each pulse from a fixed reference, is proportional to the value of the message signal at each sampling instant.
- Digital pulse modulation results when the sample values of the message signal are quantized and encoded prior to transmission.
- A convenient measure of bandwidth occupancy for digital modulation is in terms of out-of-band power or power-containment bandwidth. An ideal brick wall containment bandwidth that passes 90% of the signal power is approximately  $1/T_b$  Hz for QPSK, OQPSK, and MSK and about  $2/T_b$  Hz for BPSK
- Phase Shift Keying is often used, as it provides a highly bandwidth efficient modulation scheme.
- QPSK, modulation is very robust, but requires some form of linear amplification. QPSK and  $\pi/4$ -QPSK can be implemented, and reduce the envelope variations of the signal.
- High level M-ary schemes (such as 64-QAM) are very bandwidth efficient, but more susceptible to noise and require linear amplification.
- Constant envelope schemes (such as GMSK) can be employed since an efficient, non-linear amplifier can be used.
- Coherent reception provides better performance than differential, but requires a more complex receiver.

## 5.6 EXERCISES

1. Consider a four-phase PSK signal represented by the equivalent low-pass signal

$$u(t) = \sum_n I_n g(t - nT)$$

where  $I_n$  takes on one of the four possible values  $\sqrt{\frac{1}{2}}(\pm 1 \pm j)$  with equal probability. The sequence of information symbols  $\{I_n\}$  is statistically independent.

- a. Determine and sketch the power density spectrum of  $u(t)$  when

$$g(t) = \begin{cases} A, & 0 \leq t \leq T \\ 0, & \text{otherwise} \end{cases}$$

- b. Repeat (a) when

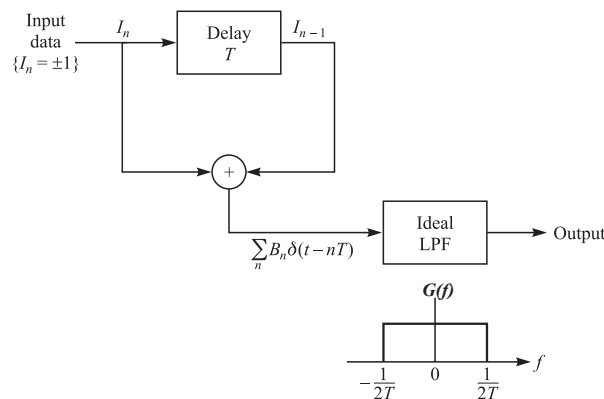
$$g(t) = \begin{cases} A \sin(\pi t/T), & 0 \leq t \leq T \\ 0, & \text{otherwise} \end{cases}$$

- c. Compare the spectra obtained in (a) and (b) in terms of the 3-dB bandwidth and the bandwidth to the first spectral zero
2.  $\pi$ - QPSK may be considered as two QPSK systems offset by  $\pi/4$  radians.
  - a. Sketch the signal space diagram for a  $\pi/4$ -QPSK signal
  - b. Using Gray encoding, label the signal points with the corresponding data bits.
3. A PAM partial-response signal (PRS) is generated as shown in Figure by exciting an ideal lowpass filter of bandwidth  $W$  by the sequence

$$B_n = I_n + I_{n-1}$$

at a rate  $1/2 T = 2W$  symbols/s. The sequence  $\{I_n\}$  consists of binary digits selected independently from the alphabet  $\{1, -1\}$  with equal probability. Hence, the filtered signal has the form

$$v(t) = \sum_{n=-\infty}^{\infty} B_n g(t - nT), T = \frac{1}{2W}$$



- a) Sketch the signal space diagram for  $v(t)$ , and determine the probability of occurrence of each symbol.
- b) Determine the autocorrelation and power density spectrum of the three-level sequence  $\{B_n\}$ .
- c) The signal points of the sequence  $\{B_n\}$ . form a Markov chain. Sketch this Markov chain, and indicate the transition probabilities among the states.
4. Determine the autocorrelation functions for the MSK and offset QPSK modulated signals based on the assumption that the information sequences for each of the two signals are uncorrelated and zero-mean.
5. Let  $\{a_n\}_{n=-\infty}^{\infty}$  denote an information sequence of independent random variables, taking values of  $\pm 1$  with equal probability. A QPSK signal is generated by modulating a rectangular pulse shape of duration  $2T$  by even and odd indexed  $a_n$ 's to obtain the in-phase and quadrature components of the modulated signal. In other words, we have

$$g_{2T}(t) = \begin{cases} 1, & 0 \leq t \leq 2T \\ 0, & \text{otherwise} \end{cases}$$

and we generate the in-phase and quadrature components according to

$$x_i(t) = \sum_{n=-\infty}^{\infty} a_{2n} g_{2T}(t - 2nT)$$



$$x_q(t) = \sum_{n=-\infty}^{\infty} a_{2n+1} g_{2T}(t - 2nT)$$

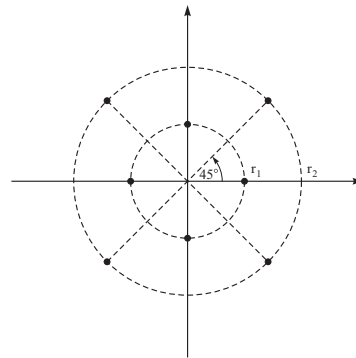
Then  $x_l(t) = x_i(t) + jx_q(t)$  and  $x_l(t) = \text{Re}[x_l(t)e^{j2\pi f_0 t}]$

- a) Determine the power spectral density of  $x_l(t)$ .
- b) Now let  $x_q(t) = \sum_{n=-\infty}^{\infty} a_{2n+1} g_{2T}(t - (2n + 1)T)$ , in other words, let the quadrature component stagger the in-phase component by  $T$ . This results in an OQPSK system. Determine the power spectral density of  $x_l(t)$  in this case. How does this compare with the result of part a?
- c) If in part b instead of  $g_{2T}$  we employ the following sinusoidal signal

$$g_1(t) = \begin{cases} \sin\left(\frac{\pi t}{2T}\right), & 0 \leq t \leq 2T \\ 0, & \text{otherwise} \end{cases}$$

the resulting modulated signal will be an MSK signal. Determine the power spectral density of  $x_l(t)$  in this case.

- d) Show that in the case of MSK signaling, although the basic pulse  $g_1(t)$  does not have constant amplitude, the overall signal has a constant envelope.
6. Consider the signal constellation shown in Figure



The lowpass equivalent of the transmitted signal is represented as

$$s_l(t) = \sum_{n=-\infty}^{\infty} a_n g(t - nT)$$

where  $g(t)$  is a rectangular pulse defined as

$$g(t) = \begin{cases} 1, & 0 \leq t < T \\ 0, & \text{otherwise} \end{cases}$$

and the  $a_n$ 's are independent and identically distributed (iid) random variables that can assume the points in the constellation with equal probability.

- a) Determine the power spectral density of the signal  $s_1(t)$ .
- b) Determine the power spectral density of the transmitted signal  $s(t)$ , assuming that the carrier frequency is  $f_0$  (assuming  $f_0 \gg \frac{1}{T}$ ).
- c) Determine and plot the power spectral density of  $s_1(t)$ . for the case when  $r_1 = r_2$  (plot the PSD as a function of  $f T$ ).

